

## Development of a personalized parametric finite element model of the knee: Evaluation of geometric variables affecting osteoarthritis progression

Fatemeh Abdollahpour<sup>a</sup>, Goldis Darbemamieh<sup>a,\*</sup>, Mohammad Nikkhoo<sup>b,c</sup>, Kamran Hassani<sup>d,e</sup>, Sadegh Rahmati<sup>a</sup>

<sup>a</sup> Department of Biomedical Engineering, Central Tehran Branch, Islamic Azad University, Tehran, Iran

<sup>b</sup> School of Physical Therapy and Graduate Institute of Rehabilitation Science, College of Medicine, Chang Gung University, Taoyuan, Taiwan

<sup>c</sup> Bone and Joint Research Center, Chang Gung Memorial Hospital, Linkou, Taiwan

<sup>d</sup> Department of Biomedical Engineering, Science and Research Branch, Islamic Azad University, Tehran, Iran

<sup>e</sup> School of Mechanical, Industrial and Aeronautical Engineering, Witwatersrand University, Johannesburg, South Africa

### ARTICLE INFO

#### Keywords:

Personalized  
Finite element analysis  
Knee osteoarthritis  
Geometrical parameters  
Stress

### ABSTRACT

**Background:** Osteoarthritis is a degenerative condition that impacts synovial joints, particularly the knee joint. Researchers regard Finite Element Analysis as a promising technique for managing knee osteoarthritis. However, these models often depend on input geometry from one or more individuals, feature complex interfaces, and require a significant amount of time, which makes them unsuitable for clinical use and reduces their reliability.

**Purpose:** This study aims to assess the effectiveness of the personalized parametric model technique in predicting the knee joint's mechanical response, taking into account anatomical variables that influence osteoarthritis.

**Methods:** A 3D model of the knee was created from CT images of a patient with knee osteoarthritis. Lateral, anterior, and posterior knee radiographs were obtained from twenty-six subjects to customize the geometric parameters of the developed parametric model. The knee geometry was parameterized using Ansys software. The models used six parameters to represent the articular surface of the tibial plateau, its slope, and variables attached to the medial and lateral femoral condyles. Parametric FE models were created individually by applying the ground reaction force diagram to each model.

**Results:** Mean maximum von Mises stress was higher in the OA group than in the control group. Simulations of the patients in the OA group indicated that the mean von Mises stress at the articular surfaces diminished with an increase in tibial plateau tilt. Also, individual geometry-specific models exhibited varying responses, thereby confirming the significance of taking personalized geometry into account.

**Conclusion:** Personalized models can be used to simulate mechanical responses and specifically evaluate the effect of the tibial plateau tilt. This work presented an innovative method for creating individualized finite element models of osteoarthritic knees, which can be used as a practical and effective tool in clinical environments.

### 1. Introduction

Osteoarthritis (OA) is a degenerative condition that diminishes the mechanical characteristics of articular cartilage and bone. OA is a significant public health issue because it causes pain, incapacity, and incurs substantial expenses.<sup>1</sup> Furthermore, the knee joint has the highest occurrence rate among all anatomical joints.<sup>2</sup> The huge increase in the number of knee replacement surgeries, usually for severe osteoarthritis, in the past few years, especially among young people, is cause for

alarm.<sup>3</sup> Therefore, it is crucial to implement efficient interventions that focus on enhancing comprehension, control, and mitigation of related risk factors.<sup>3</sup> Knee joint osteoarthritis is influenced by various factors, including age, obesity, race, genetics, and sex hormones.<sup>4</sup> Severe joint blows and excessive pressure from work or sports are among the factors that influence knee joint osteoarthritis.<sup>5</sup> Additionally, many studies have indicated that anatomical variables may play a role in causing knee osteoarthritis.<sup>6–8</sup> Among some of the anatomical factors introduced in this regard, we can mention the tibial plateau tilt (TPT),<sup>9–11</sup> the cam

\* Corresponding author.

E-mail address: [goldis\\_emamieh@aut.ac.ir](mailto:goldis_emamieh@aut.ac.ir) (G. Darbemamieh).

effect<sup>1</sup> (CE),<sup>12–14</sup> and the tibial plateau coverage by femoral condyles (TPCFC).<sup>15,16</sup> The results of research indicated that the osteoarthritis group had greater tibial plateau curvature, cam effect, and femoral condyle coverage than the control group.<sup>17</sup> Therefore, it is hoped that these features can be used to monitor the onset and progression of osteoarthritis in individuals. A comprehensive understanding and evaluation of knee joint biomechanics are essential for improving the prediction and management of associated issues. Finite element models (FEM) are the solution to the problem. Given the lack of proven effects of these factors on biomechanical responses of the knee joint, we considered the anatomical parameters of TPT, CE, and TPCFC as customizable parameters in the parametric model developed for this study. Therefore, in order to investigate the influence of anatomical parameters on the biomechanical responses of the knee joint, we created a parametric finite element model.

Finite element models has gained prominence in recent decades as a useful and practical approach for doing non-invasive biomechanical research on the knee.<sup>18</sup> FEM have been employed to evaluate hypotheses concerning the mechanisms of osteoarthritis at various scales. Researchers have examined the impact of the depletion of cartilage components on the mechanical response of tissue, including reaction forces and displacements during unconfined compression relaxation tests of cartilage samples.<sup>19</sup> Others examined the intercommunication between tissues, which could facilitate tissue remodeling in response to alterations in the mechanical.<sup>20</sup> On the other hand, researchers have modeled various pathological diseases at the joint level. These studies encompass examinations of the influence of the dimensions and location of superficial cartilage defects on strain and stress concentrations,<sup>21</sup> the relative orientation of knee components on cartilage thinning.<sup>22</sup>

Typically, a finite element analysis (FEA) is conducted in three steps: a pre-processing step to build the model, a processing step to resolve the mathematical problem, and a post-processing step to analyze the results and draw conclusions. Particularly for FEA of the knee joint, the duration necessary to produce precise subject-specific models, with detailed three-dimensional (3D) geometries and FE meshes, constitutes the main challenge for clinical use, as it may require several working days per individual.<sup>23,24</sup> Prior studies have shown certain shortcomings in knee finite element models. Due to the intricate geometry of the knee, these models generally involve complicated interfaces, necessitating substantial spending time in the preprocessing, processing, and post-processing phases of finite element analysis. This renders them inappropriate for therapeutic application.<sup>25</sup> Furthermore, these models frequently rely on input geometry obtained from one or more individuals; thereby, the existence of inherent geometric variability among individuals can bring a degree of uncertainty into the conclusions of models that rely on one data, diminishing their trustworthiness.<sup>26</sup> In this study, for the first time, a customized parametric finite element model was created based on the geometric variables TPT, CE, and TPCFC to fill the current gaps that are developed. For clinical use, we created a personalized FE model that changes the knee joint’s geometry based on TPT, CE, and TPCFC factors. This was done to find out how these factors affect knee biomechanical responses in people with osteoarthritis. The development of the parametric model is anticipated to yield two primary benefits: firstly, it enhances understanding of the anatomical origins of osteoarthritis onset and progression, and secondly, it improves treatment efficacy through the more tailored design of knee prostheses for patients.

<sup>1</sup> The cam effect is a measure of the ratio between the longest diameter of the inner condyle of the femur and the height of the outer condyle of the femur<sup>17</sup>

## 2. Materials and methods

### 2.1. Human experiments

Thirteen individuals with knee arthritis and thirteen asymptomatic individuals provided laboratory measurements while they were walking. Table 1. This work has received local approval from the Ethics Committee of Islamic Azad University’s Central Tehran branch. The participants provided their informed consent to engage in this research project. Kellgren and Lawrence’s method is the criterion for dividing the two groups of control and osteoarthritis.<sup>27</sup> An anterior-posterior view in the open vault and a posterior-anterior view in the weight-bearing position with 30 degrees of knee flexion were the radiography images obtained for this study.<sup>28</sup> Ground response forces were quantified with two Kistler force plates embedded in the laboratory flooring. Mimics software was utilized to extract the geometric variables from radiographic images of individuals. Ultimately, each individual GRF, TPT, CE, and TPCFC were utilized as inputs to simulate the parametric finite element model.

### 2.2. Parametric modeling of knee joint geometry

The original geometry of the knee joint was derived from a 3D tomographic scan of a volunteer patient diagnosed with knee osteoarthritis. The initial model of the knee joint was retrieved as a point cloud from the DICOM picture, inputted into MIMICS (Materialize, Leuven, Belgium), and subsequently reverse-engineered using Geomagic Design X software. A 3D model of the knee joint was developed. Radiographs of the knee joint taken laterally, anteriorly, and posteriorly (AP) were used to measure the predetermined parameters needed for the parametric finite element model. These images were taken under the guidance of a radiologist. Then, using MIMICS software, geometric parameters were calculated for each individual.

The tibial plateau tilt (TPT) equation (1),<sup>29</sup> Cam effect (CE) using formula 2,<sup>29</sup> and we also calculated the tibial plateau coverage by femoral condyles (TPCFC) using formula 3.<sup>29</sup> The anatomical positioning of the variables  $\alpha$ , L<sub>M</sub>, H<sub>L</sub>, a, b, and c is shown in Fig. 1. The longest diameter of the inner condyle of the femur is designated as L<sub>M</sub>, and H<sub>L</sub> signifies the height of the outer condyle of the femur. The contact surfaces of the femoral condyles are designated as a and b, also the articular surface of the tibial plateau is labeled as c. Tables 2 and 3 display a comprehensive report of geometric parameters. To control interobserver and intraobserver variability, the measuring method was conducted independently by two distinct individuals and replicated three times to validate its reliability. The intraclass correlation coefficients (ICC) were computed to assess the reliability of both intra- and interobserver measurements.<sup>30</sup> The customized model can be updated by inputting new values according to the limitations and geometric relationships indicated in Table 3.

$$\alpha = 90 - \alpha' \tag{1}$$

$$\text{Cam effect} = L_M / H_L \tag{2}$$

$$\text{TPCFC} = \frac{(a + b)}{c} * 100 \tag{3}$$

The knee joint geometry was derived by reconstructing CT images of the bony structures and directly digitizing the soft tissue limiting surfaces and ligament insertion points of a female specimen with knee osteoarthritis.<sup>31</sup> This reconstruction was based on the shape of three

**Table 1**  
Demographic data pertaining to study participants.

	Age (years)	Height (cm)	Weight (kg)
OA	61.92 ± 3.43	169.238 ± 5.83	73.69 ± 6.03
CONTROL	60.154 ± 2.71	170.951 ± 7.45	71.31 ± 5.61

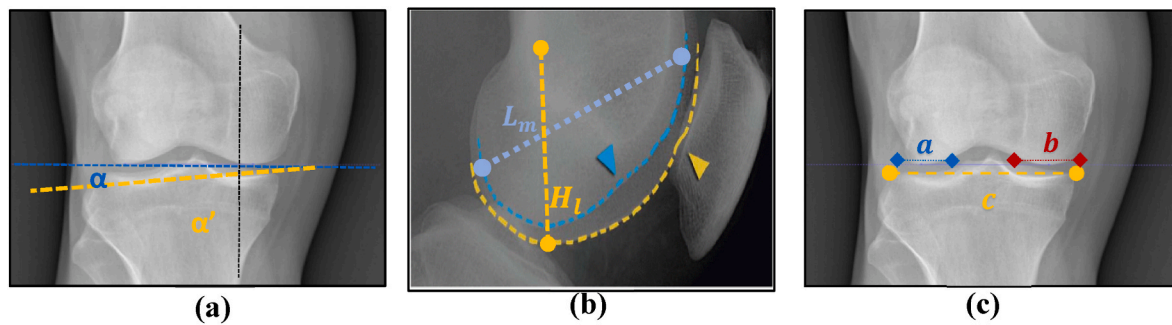


Fig. 1. A view of personalized geometries obtained from radiographic images of subjects. 1.a: Calculating the tibial plateau tilt (TPT) from the radiographic images of the subject's knee joint 1.b: Calculating the Cam effect (CE); 1.c: Calculating the tibial plateau coverage by femoral condyles (TPCFC).

**Table 2**  
Anatomical characteristics affecting knee osteoarthritis simulated in parametric finite element models.

FE Model	OA Group			Control Group		
	TPT (degree)	CE	TPCFC (%)	TPT (degree)	CE	TPCFC (%)
Model No. 1	14.67	1.86	53.12	10.27	1.75	49.36
Model No. 2	12.53	1.94	54.41	11.14	1.82	50.29
Model No. 3	9.48	1.79	49.93	11.93	1.86	51.66
Model No. 4	12.03	1.92	52.56	10.71	1.76	50.84
Model No. 5	11.82	1.88	50.66	12.76	1.94	51.61
Model No.6	8.07	1.76	47.34	13.66	1.92	52.16
Model No.7	10.39	1.85	49.26	10.58	1.77	48.31
Model No.8	12.92	1.89	53.77	10.97	1.78	49.75
Model No.9	10.44	1.78	47.23	11.65	1.85	51.33
Model No.10	14.16	1.92	55.03	8.27	1.59	46.47
Model No.11	11.79	1.83	51.11	9.57	1.65	47.68
Model No. 12	13.23	1.91	52.36	10.86	1.75	48.77
Model No. 13	13.83	2.03	58.23	7.91	1.56	46.59

bones (tibia, patella, and femur), their articular cartilage layers, the meniscus, and four ligaments (ACL, PCL, LCL, and MCL in TF).<sup>32</sup> Furthermore, it included the longest diameter of the inner condyle of the femur ( $L_m$ ), the longest height of the outer condyle of the femur ( $H_l$ ), the contact surface of the inner and outer condyles of the femur (a, b), and the articular surface of the tibial plateau (c).<sup>29,33</sup> The knee geometry was parametrized using Ansys software in the lower femur, upper tibia, menisci, and cartilages. Six parameters were used in the models to represent the tibial plateau's articular surface, its tilt, and variables connected to the femur's medial and lateral condyles (Fig. 2). Based on the defined geometric constraints and relationships, the geometric parametric model can be adjusted automatically by entering new values for each of the above parameters. To build a simple geometric model, our main goal is to reduce the number of parameters as much as possible based on the parsimony principle. To do this, we first performed a series of sensitivity analyses on the moving parts to see how different parameters affect the biomechanical parameters. The geometric parameters of TPT, CE, and TPCFC (Table 2) of the knee were considered. The dimensions defined in Fig. 2 are based on the maximum fit of the model with the CT scan images.

Parametric FE models were created individually by applying the ground reaction force diagram to each model (Fig. 2b) based on the values of the six parameters  $\alpha$ ,  $L_m$ ,  $H_l$ , a, b, and c (Table 3) (Fig. 2).<sup>34</sup> Each parametric FE knee model consisted of three bones (tibia, patella, and femur), articular cartilage, meniscus, and four ligaments (ACL, PCL, LCL, and MCL in TF). The material properties were defined as shown in Table 4. The meniscus was considered orthotropic,<sup>20</sup> the ligaments were considered Neo-Hookean hyper elastic,<sup>35</sup> and the articular cartilage was

**Table 3**  
Customized geometry factor in parametric finite element model.

FE Model	OA Group						Control Group					
	$\alpha$	$L_m$	$H_l$	a	b	c	$\alpha$	$L_m$	$H_l$	a	B	c
No. 1	75.33	87.36	46.97	76.22	79.40	292.97	79.73	78.99	45.13	72.20	75.51	299.24
No. 2	77.47	89.41	46.09	78.27	81.46	293.56	78.86	82.77	45.49	75.99	79.30	308.81
No. 3	80.52	84.98	47.47	73.83	77.02	302.13	78.07	83.89	45.11	77.11	80.41	304.91
No. 4	77.97	86.92	45.27	75.78	78.97	294.43	79.29	78.37	44.53	71.57	74.88	288.07
No. 5	78.18	92.37	49.13	81.22	84.41	326.96	77.24	84.36	43.49	77.57	80.88	307.02
No.6	81.93	86.17	48.96	75.03	78.21	323.72	76.34	85.28	44.42	78.49	81.79	307.29
No.7	79.61	88.26	47.71	77.12	80.30	319.57	79.42	77.32	43.69	70.53	73.84	298.85
No.8	77.08	90.23	47.74	79.09	82.28	300.10	79.03	78.63	44.18	71.84	75.15	295.47
No.9	79.56	82.79	46.51	71.64	74.83	310.13	78.35	80.32	43.42	73.53	76.84	292.95
No.10	75.84	91.09	47.44	79.94	83.13	296.33	81.73	74.33	46.75	67.54	70.84	297.78
No.11	78.21	89.16	48.72	78.01	81.2	311.51	80.43	75.51	45.77	68.72	72.03	295.19
No. 12	76.77	90.79	47.54	79.65	82.84	310.34	79.14	79.41	45.38	72.62	75.92	304.59
No. 13	76.17	93.57	46.09	82.42	85.61	288.57	82.09	75.57	48.44	68.78	72.08	302.34

( $\alpha$  in degrees and a, b, c,  $L_m$  and  $H_l$  in millimeters).

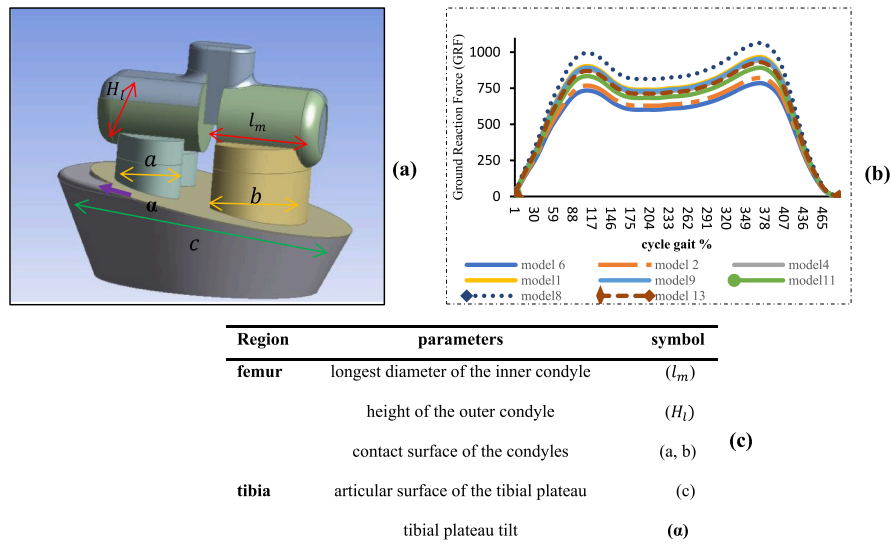


Fig. 2. 2.a: customized finite element modeling method of knee joint, 2.b: ground reaction force diagram for models, 2.c: Selected parameters for knee joint generation.

considered Neo-Hookean hyper elastic.<sup>36</sup> Also, the cancellous and cortical bones were defined as orthotropic.<sup>37</sup>

### 2.3. Material properties

The properties were considered as Neo-Hookean hyper elastic isotropic materials for a non-fibrillar solid matrix of cartilage layers, with a linear elastic modulus of 2.55 MPa and a Poisson’s ratio of 0.45. The Convergence Challenge necessitated the utilization of this approach.<sup>36</sup> The Menisci matrix has values of  $E11 = 4.65$ ,  $E22 = 4.65$ , and  $E33 = 138$  MPa for the elastic modulus, and  $G12 = 1.0575$ ,  $G13 = 1.95$ , and  $G23 = 1.9$  MPa for the shear modulus.<sup>20</sup> Additionally, the Poisson’s ratio values of  $V12 = 0.843$ ,  $V13 = 0.022$ , and  $V23 = 0.0276$  indicate that the matrix is orthotropic (non-isotropic) elastic.<sup>20</sup> The Neo-Hookean hyper elastic model was employed to simulate the ACL, PCL, LCL, and MCL ligaments, which were only activated in the stretch mode.<sup>35</sup> (Table 4).

### 2.4. Loading, kinematics, and boundary conditions

To prepare the model for finite element analysis, the GRF force corresponding to each patient (Fig. 2b) was applied to the upper surface of the femur.<sup>38</sup> Additionally, in order to define the boundary conditions for the analysis, the lower surface of the tibia bone was considered completely constrained (Fig. 3e).<sup>31</sup> The next step was to discretize the geometric model and create a network within it. The model’s meshing was done in a tetrahedral type. Finally, for each model, the total number of elements was 21222, and the total number of nodes was 43329. Fig. 3f shows an image of the finite element model that has been created. In each subject and according to TPT, CE, and TPCFC geometric factors, GRF and body weight, von Mises stress in the knee joint was predicted. To ascertain the congruence of the model results with previously documented data in numerical research, the maximum stress of the joint contact surface derived from the parametric model was ultimately compared with numerical studies.<sup>39,40</sup>

### 3. Results

Good average intra-observer reliability ( $ICC = 0.826$ ) and inter-observer reliability ( $ICC = 0.739$ ) were attained. The knee joint geometry was correctly reconstructed in the pictures for all patients. Subsequently, individualized finite element models for each patient were

constructed, and their accuracy was verified by mesh sensitivity analysis. The average von Mises stress values were consistent with those reported in prior research (Fig. 4).<sup>18,39,40</sup> The von Mises stress distribution estimated from the parametric finite element model was shown in the osteoarthritis group (Fig. 5) and the control group (Fig. 6).

The mean maximum Von Mises stress in the OA group exceeds that of the control group. This is true when examining the impacts of all three anatomical parameters. Furthermore, the H-TPT, M-CE, and H-TPCFC groups demonstrated the highest levels of Von Mises stress in comparison to the other two categories (Fig. 7).

### 4. Discussion

Examining the biomechanical characteristics of the knee is essential for comprehending the mechanical elements that lead to osteoarthritis. This understanding may facilitate the formulation of measures to prevent or alleviate the adverse effects of OA. This work presented an innovative method for creating individualized finite element models of osteoarthritic knees, which can be used as a practical and effective tool in clinical environments. The results produced from the novel parametric model were compared to previous studies accurate models, revealing similar biomechanical responses.<sup>18,39,41,42</sup> However, in the parametric model, the values for the calculated Von Mises stress were higher. This is likely due to the use of geometry simplification techniques adopted from the literature.<sup>43</sup> These techniques employed flat surfaces instead of concave or convex surfaces to mimic the joints.<sup>43</sup>

This work involved the customization of a parametric finite element model based on data obtained from X-ray pictures. X-ray imaging is a commonly utilized and readily available technique that is more cost-effective than MRI and CT.<sup>44</sup> Despite the evident advantages of CT scanning, its use is constrained by radiation exposure and the fact that it is frequently conducted with the patient in a supine position, which cannot reflect the different body positions during normal everyday activities.<sup>45</sup> Clinical application was another important goal of our research. It involves detailed mechanical response and parameter extraction processes performed by clinicians with no prior knowledge. After training, the measurement procedure was performed by two different people independently and repeated three times, with good intra- and inter-observer reliability. The knee joint values were extracted in less than 15 min. Importantly, the FE model used in this study demonstrated that it can be constructed automatically by users in clinics inputting parameter values, even if they have no programming or FE

**Table 4**  
Mechanical properties of the parametric finite element model.

Knee Component	Material Behavior	Mechanical Properties	References
meniscus	Orthotropic elastic	Elastic modulus (MPa) E11 = 6.2, E22 = 6.2, E33 = 184 Shear modulus (MPa) G12 = 1.41, G13 = 2.6, G23 = 2.6 Poisson's ratio ν12 = 0.917, ν13 = 0.024, ν23 = 0.03	20
Ligaments	Neo-Hookean Hyper elastic	ACL: C10 = 1.95, D1 = 0.00683 PCL: C10 = 3.24, D1 = 0.0042 LCL: C10 = 1.45, D1 = 0.00127 MCL: C10 = 1.45, D1 = 0.0012	35
Articular cartilage	Neo-Hookean Hyper elastic	Elastic modulus (MPa) 4.4 Poisson's ratio 0.49	36
spongy bone	Orthotropic elastic	Elastic modulus (MPa) E11 = 1352, E22 = 968, E33 = 676 Shear modulus (MPa) G12 = 292, G13 = 505, G23 = 370 Poisson's ratio ν12 = 0.30, ν13 = 0.30, ν23 = 0.30	37
Cortical bone:	Orthotropic elastic	Elastic modulus (GPa) E11 = 16, E22 = 6.88, E33 = 6.30 Shear modulus (GPa) G12 = 3.20, G13 = 3.30, G23 = 3.60 Poisson's ratio ν12 = 0.30, ν13 = 0.30, ν23 = 0.45	37

ACL: The anterior cruciate ligament PCL: The posterior cruciate ligament LCL: The lateral collateral ligament MCL: The medial collateral ligament.

modeling expertise. The primary advantage of the parametric modeling approach presented in this study is its ability to significantly streamline the process of personalizing geometrical features, thereby reducing the computational time required. The reconstruction of precise geometric knee joint surfaces from CT scan images using standard image processing software, along with the development of complete and accurate finite element models while solving numerical errors, is typically a time-consuming task.<sup>46</sup> In contrast, this study presents a built parametric model that can be swiftly regenerated for each individual using extracted parameters from X-ray pictures in approximately 40 min. A recent study demonstrated a method for automatically generating finite element meshes of knee joints using computed tomography (CT).<sup>47</sup> However, the problem with this technique, which automatically creates a mesh based on CT scan images, is the immutability of the model. Changing the geometry to mimic different knee joint injuries or therapy manipulations is a significant advantage. In this study, we were able to change some geometric details in the model using parametric modeling for each individual. Although simplified geometry has its limitations, personalized parametric modeling has the potential to overcome these constraints and serve as a noninvasive and cost-effective technique for evaluating differences in knee joint geometry and alignment in clinical

settings using FE simulations.

Results found that individual geometry-specific models exhibited varying responses, thereby confirming the significance of taking personalized geometry into account (Figs. 4–7). Osteoarthritis, which can occur at any level of the knee, might potentially lead to biomechanical changes in the joint surfaces and associated tissues. While there are no published results that could be directly compared with the results obtained from this model, the increase in maximum von Mises stresses in OA groups compared to the control group is acceptable based on projections in the literature<sup>39</sup> (Figs. 4 and 7). In this study, the impact of TPT, CE, and TPCFC on the biomechanics of the knee joint was examined. For each parameter, three distinct circumstances were examined in both groups of individuals. Simulations of the patients in the OA group indicated that the mean von Mises stress at the articular surfaces diminished with an increase in tibial plateau tilt, but it escalated with higher CE and TPCFC values, except for the von Mises stress in the M-CE category. This indicates that these outcomes are contingent upon the individual geometry. Hence, the advantage of the method provided here is that the biomechanical responses, which may be examined for patients under different clinical interventions, are not limited by a specific geometry. For instance, the assessment of the posterior tilt angle of the tibial prosthesis is essential in knee arthroplasty and influences its longevity and clinical effectiveness.<sup>48</sup> Despite the growing sophistication of arthroplasty surgical equipment, the determination of the final osteotomy angle and prosthesis positioning predominantly depends on the surgeon's expertise. Nonetheless, tibial plateau tilt is closely associated with knee bone structural stress, ligament tension, kinematics, and platform wear rate; thus, establishing the optimal tibial plateau tilt angle remains contentious.<sup>49</sup> Therefore, pertinent biomechanical investigations with elevated precision and predictability are essential.

The overarching trend of variations in Von Mises equivalent stress within the simulated parametric finite element models is as follows: The largest tilt of the tibial plateau is attributed to the H-TPT group, which exhibits a tilt of 12.5° or greater as assessed from X-ray scans of the individuals. There is lower von Mises stress in models 1, 2, 8, 10, 12, and 13 in the H-TPT group than in models 4, 5, 7, and 11 in the M-TPT group, whose tibial plateau tilt is measured to be between 10.5 and 12.5°. The results indicated that the von Mises stress in the L-TPT group, which has a simulated tibial plateau slope of less than 10.5°, exceeds that of the M-TPT group. Augmenting the tilt of the tibial plateau reduces the von Mises stress (Fig. 7), suggesting that the von Mises stress is contingent upon the geometric parameters of the individuals. This phenomenon can be explained by the progressive elevation of the posterior tilt of the tibial plateau from 8° to 14°, alongside the concomitant reduction in stress exerted on the parametric models of the knee joint and the tibial plateau surface. The highest von Mises stress pertains to models exhibiting a simulated cam effect ranging from 50.5 to 52.5, as determined from models (1-5-7-8-11). The findings indicated that the estimated von Mises stress from models (1-2-4-8-10-13) in group H-TPCFC, which exhibits a tibial plateau surface occupation by femoral condyles exceeding 52.5 %, is greater than that observed in groups M-TPCFC and L-TPCFC, which have a lower tibial plateau surface occupation by femoral condyles. This suggests that a higher degree of tibial plateau occupation by femoral condyles results in elevated von Mises stress. This may result from heightened wear on the contact surface. In the future, personalized models will enable the calculation of the optimal occupation surface by condyles, facilitating the creation of knee prostheses that exert minimal stress on the contact surface, hence enhancing clinical efficiency and prolonging the prosthesis lifespan for individuals.

This study provided a platform for clinical biomechanical analyses of knee joints for specific patients. The results (Figs. 4 and 7) showed that individual patient geometry can influence the biomechanical response. For example, the present results suggest that increasing the tibial plateau surface occupation by femoral condyles may create a more uneven stress distribution by increasing the stress concentration in the H-TPCFC category, leading to a potential increase in the risk and rate of OA onset.

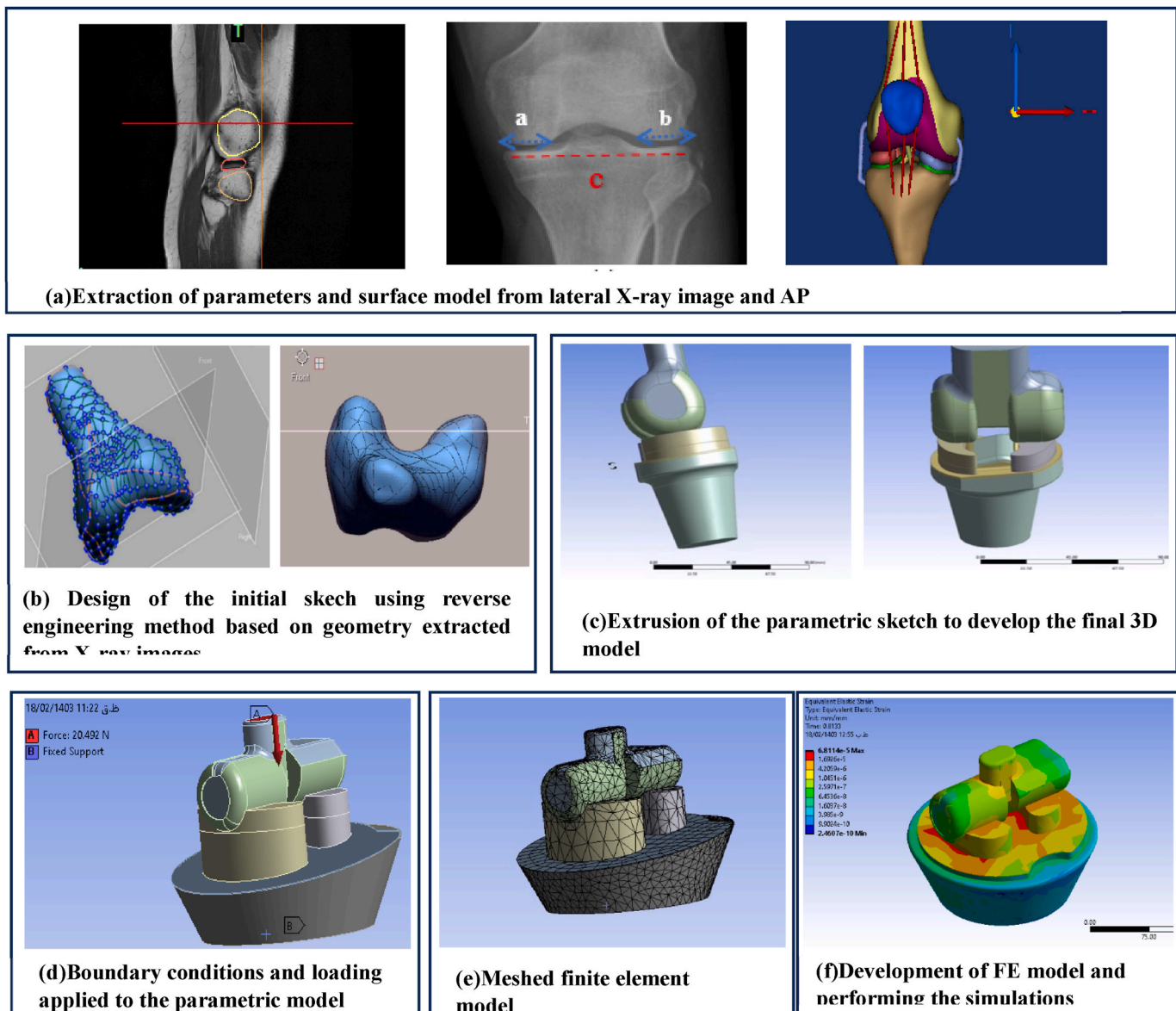


Fig. 3. Steps to create a customized finite element model for the knee joint.

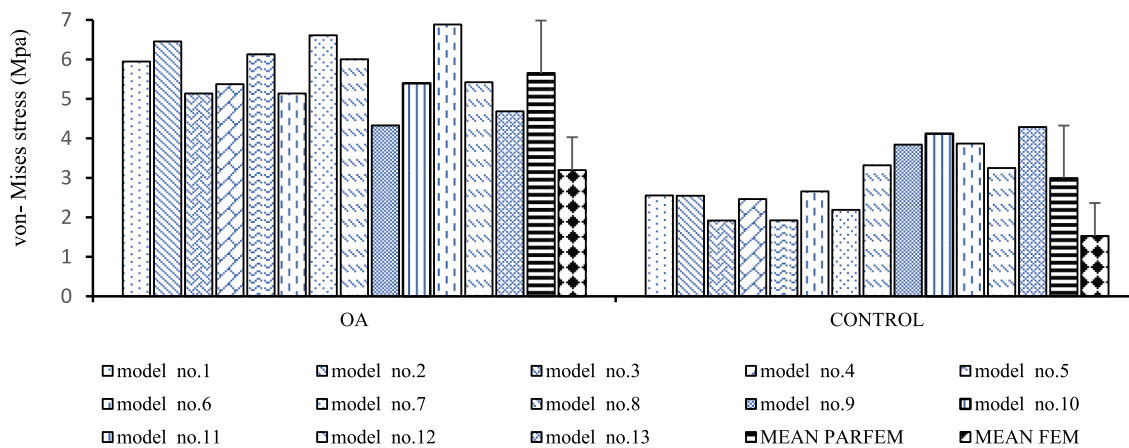


Fig. 4. Comparison of von Mises stress in parametric models with personalized geometric parameters for the subjects of both groups and comparison of the average predicted stress of our parametric model with previous studies.<sup>39</sup>

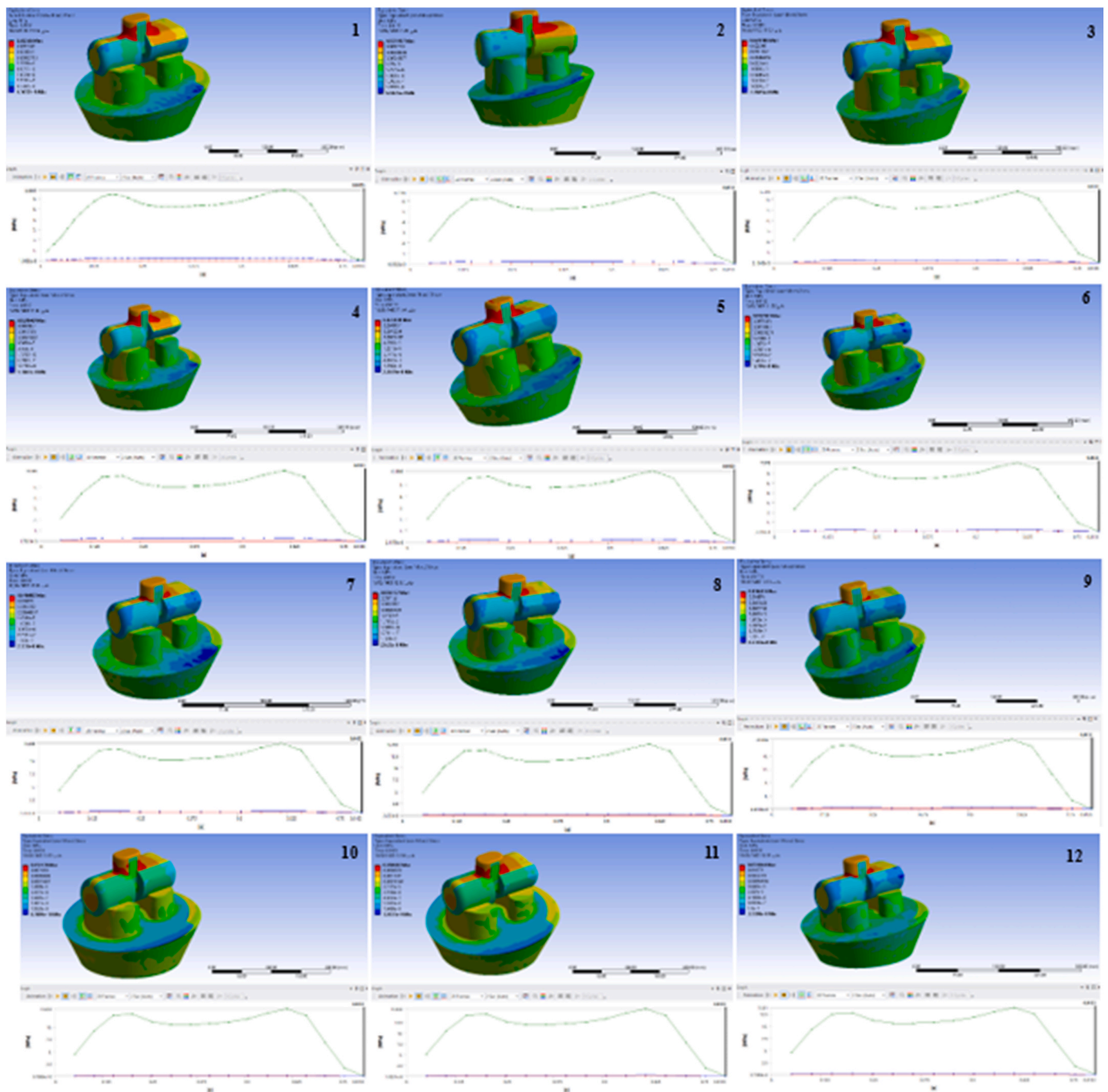


Fig. 5. Estimated von Mises stress distribution from twelve personalized parametric finite element models in the osteoarthritis group (subject no. 1 to 12).

This suggests that AO disrupts stress throughout the structure, potentially reducing overall biomechanical stability. The increase in peak stress concentration in the AO group may heighten the risk of fracture or local damage, suggesting that AO negatively impacts biomechanical performance.<sup>42</sup> This is in accordance with clinical observations that confirm a strong correlation between TPCFC and the development of OA.<sup>17,29</sup> However, each individual or patient typically has a different optimal slope.<sup>49</sup> The increased stress levels in the OA group indicate weakening of material properties or structural integrity, which is probably due to changes in the normal knee structure and anatomical parameters of TPT, CE, and TPCFC.<sup>50</sup>

We must discuss some limitations of this study. Most importantly, as is characteristic of parametric modeling, this study used a combination of simple geometries to develop a model applicable to clinical settings.

Therefore, the influence of precise geometry was ignored. The second constraint arises from the assumption of consistent mechanical properties across many individuals. This inescapable barrier arises from the complexity of directly obtaining the mechanical characteristics of rigid and soft tissue from X-ray pictures. Here, we attempted to develop a pre-existing material update algorithm in order to assess the practicality of extracting personalized material attributes. Furthermore, the sample size of thirteen participants in each group limits the generalizability of the findings. Future research should focus on confirming these results through larger clinical trials and experimental studies.

**Consent to participate**

Written Informed consent was obtained from all individual

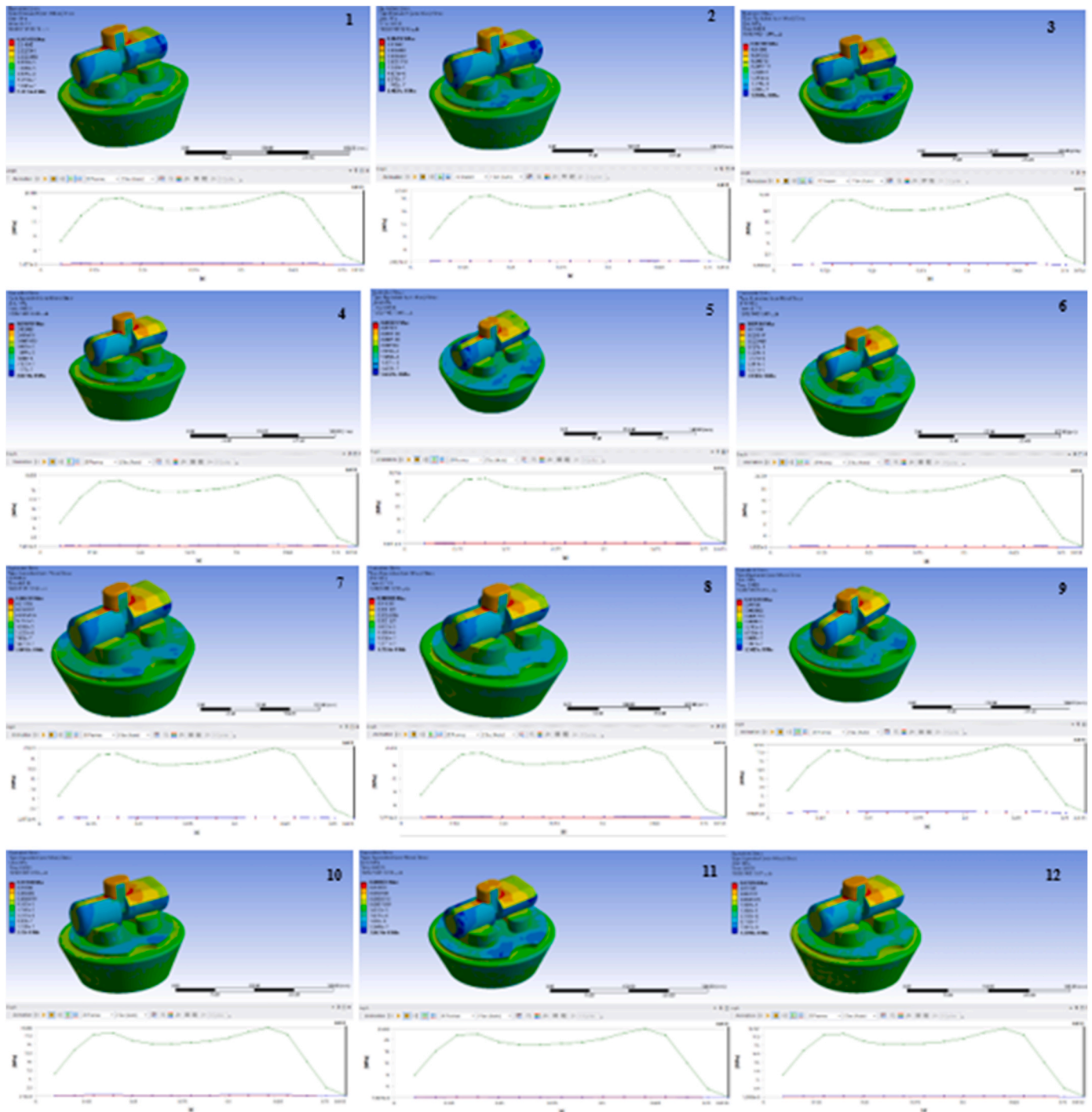


Fig. 6. Estimated von Mises stress distribution from twelve personalized parametric finite element models in the control group (subject no. 1 to 12).

participants included in the study.

**Consent to publish**

The authors affirm that human research participants provided informed consent for publication of the images and data.

**Author contributions**

All authors contributed to the study conception and design. All authors read and approved the final manuscript. All authors satisfy the criteria for authorship as outlined by the International Committee of

Journal Editors.

**Ethics approval**

This study was performed in line with the principles of the Declaration of Helsinki. It has local Approval by the Ethics Committee of University Islamic Azad University, Central Tehran branch.

**Funding**

The authors declare that no funds, grants, or other support were received during the preparation of this manuscript.

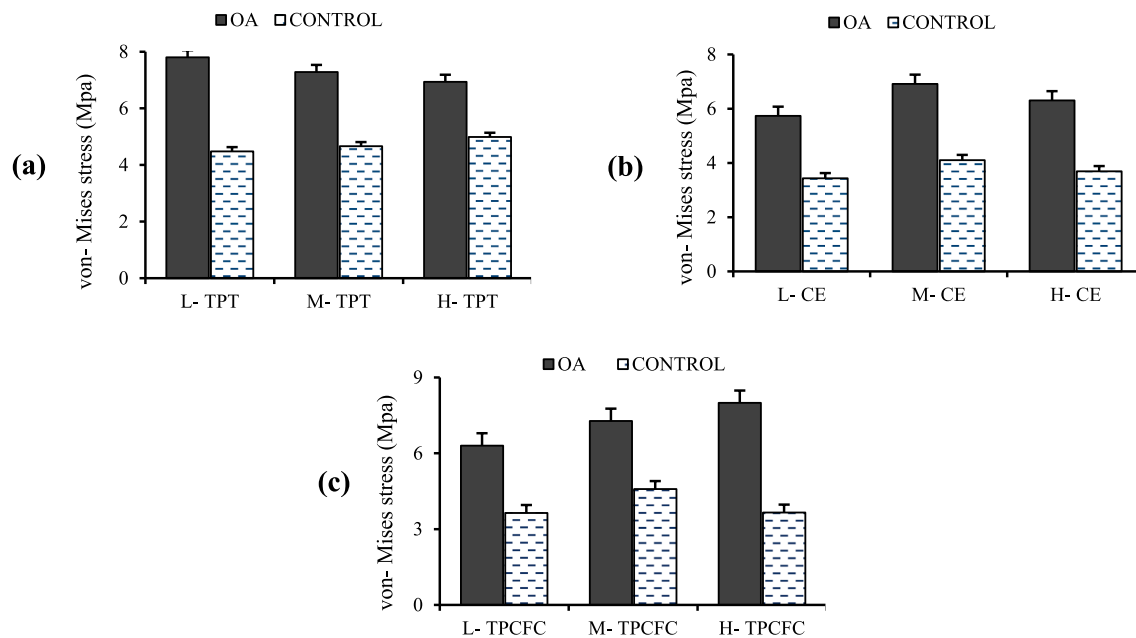


Fig. 7. Comparison of von Mises stress in customized geometric parameters between two control and osteoarthritis groups. The parameter ranges were divided into three categories: (L-TPT<10.5,10.5≤M-TPT<12.5, H-TPT≥12.5), (L-CE<1.8,1.8≤M-CE<1.9, H-CE≥1.9), and (L-TPCFC<50.5,50.5≤ M-TPCFC<52.5, H-TPCFC ≥52.5).

**Competing interests**

The authors have no relevant financial or non-financial interests to disclose.

**Acknowledgement**

All authors have reviewed the manuscript and approved its submission. This study was conducted ethically and has no conflict of interest to declare.

**Glossary**

symbol	explanation
OA	Osteoarthritis
TPT	the tibial plateau tilt
CE	cam effect
TPCFC	the tibial plateau coverage by femoral condyles
FEM	Finite element model

**References**

- Leifer VP, Katz JN, Losina E. The burden of OA-health services and economics. *Osteoarthr Cartil.* 2022;30:10–16.
- Allen KD, Thoma LM, Golightly YM. Epidemiology of osteoarthritis. *Osteoarthr Cartil.* 2022;30:184–195.
- Ackerman IN, Kemp JL, Crossley KM, Culvenor AG, Hinman RS. Hip and knee osteoarthritis affects younger people, too. *J Orthop Sports Phys Ther.* 2017;47:67–79.
- Vina ER, Ran D, Ashbeck EL, Ratzlaff C, Kwok CK. Race, sex, and risk factors in radiographic worsening of knee osteoarthritis. *Semin Arthritis Rheum. Elsevier.* 2018; 464–471.
- Orozco GA, Tanska P, Florea C, Grodzinsky AJ, Korhonen RK. A novel mechanobiological model can predict how physiologically relevant dynamic loading causes proteoglycan loss in mechanically injured articular cartilage. *Sci Rep.* 2018;8, 15599.
- Hunter DJ, Zhang Y, Niu J, et al. Structural factors associated with malalignment in knee osteoarthritis: the Boston osteoarthritis knee study. *J Rheumatol.* 2005;32: 2192–2199.
- Baker-LePain JC, Lane NE. Role of bone architecture and anatomy in osteoarthritis. *Bone.* 2012;51:197–203.
- Heijink A, Gomoll AH, Madry H, et al. Biomechanical considerations in the pathogenesis of osteoarthritis of the knee. *Knee Surg Sports Traumatol Arthrosc.* 2012; 20:423–435.
- Yoshioka Y, Siu DW, Scudamore RA, Cooke TDV. Tibial anatomy and functional axes. *J Orthop Res.* 1989;7:132–137.
- Xie K, Han X, Jiang X, et al. The effect of varus knee deformities on the ankle alignment in patients with knee osteoarthritis. *J Orthop Surg Res.* 2019;14:1–7.
- Zhang P, Wang Y-L, Liu L, Yang H-Q, Han P-F, Li X-D. Biomechanical finite element analysis of various tibial plateau posterior tilt angles in medial unicompartmental knee arthroplasty. *Exp Ther Med.* 2024;28:353.
- Mascarenhas VV, Rego P, Dantas P, et al. Can we discriminate symptomatic hip patients from asymptomatic volunteers based on anatomic predictors? A 3-dimensional magnetic resonance study on cam, pincer, and spinopelvic parameters. *Am J Sports Med.* 2018;46:3097–3110.
- Ng KCG, Lamontagne M, Jeffers JRT, Grammatopoulos G, Beaulé PE. Anatomic predictors of sagittal hip and pelvic motions in patients with a cam deformity. *Am J Sports Med.* 2018;46:1331–1342.
- Li R, Yuan X, Fang Z, Liu Y, Chen X, Zhang J. A decreased ratio of height of lateral femoral condyle to anteroposterior diameter is a risk factor for anterior cruciate ligament rupture. *BMC Musculoskelet Disord.* 2020;21:1–6.
- Babacan S, Kafa IM. Morphometric analysis of tibial plateau for knee arthroplasty and prosthesis design: morphometric analysis of tibial plateau. *Int J Curr Med Biol Sci.* 2022;2:57–63.
- Figgie 3rd HE, Goldberg VM, Heiple KG, Moller 3rd HS, Gordon N. The influence of tibial-patellofemoral location on function of the knee in patients with the posterior stabilized condylar knee prosthesis. *JBJS.* 1986;68:1035–1040.

17. Dehghan M, Bahmani M. Anatomical parameters associated with osteoarthritis of the knee joint. *Armaghane Danesh [Internet]*. 2014;19:462–469. Available from: <http://armaghanj.yums.ac.ir/article-1-183-en.html>.
18. Yan M, Liang T, Zhao H, et al. Model properties and clinical application in the finite element analysis of knee joint: a review. *Orthop Surg*. 2024;16:298–302.
19. Korhonen RK, Laasanen MS, Töyräs J, et al. Comparison of the equilibrium response of articular cartilage in unconfined compression, confined compression and indentation. *J Biomech*. 2002;35:903–909.
20. Simkheada T, Orozco GA, Korhonen RK, Tanska P, Mononen ME. Comparison of constitutive models for meniscus and their effect on the knee joint biomechanics during gait. *Comput Methods Biomech Biomed Eng*. 2023;26:2008–2021.
21. Peña E, Calvo B, Martínez MA, Doblaré M. Effect of the size and location of osteochondral defects in degenerative arthritis. A finite element simulation. *Comput Biol Med*. 2007;37:376–387.
22. Andriacchi TP, Briant PL, Bevell SL, Koo S. Rotational changes at the knee after ACL injury cause cartilage thinning. *Clin Orthop Relat Res*. 2006;442:39–44.
23. Cooper RJ, Wilcox RK, Jones AC. Finite element models of the tibiofemoral joint: a review of validation approaches and modelling challenges. *Med Eng Phys*. 2019;74:1–12.
24. Rodríguez-Vila B, Sánchez-González P, Orpessa I, Gomez EJ, Pierce DM. Automated hexahedral meshing of knee cartilage structures—application to data from the osteoarthritis initiative. *Comput Methods Biomech Biomed Eng*. 2017;20:1543–1553.
25. Du M, Sun J, Liu Y, et al. Tibio-femoral contact force distribution of knee before and after total knee arthroplasty: combined finite element and gait analysis. *Orthop Surg*. 2022;14:1836–1845.
26. Gerus P, Sartori M, Besier TF, et al. Subject-specific knee joint geometry improves predictions of medial tibiofemoral contact forces. *J Biomech*. 2013;46:2778–2786.
27. Kellgren JH, Lawrence JS. RADIOLOGICAL assessment of OSTEO-ARTHRITIS ann rheum dis. *Ann rheum Dis [Internet]*; 1957:494–503, 1956 <http://ard.bmj.com/>.
28. Sun X, Yang B, Xiao S, et al. Effect of limb rotation on radiographic alignment measurement in mal-aligned knees. *Biomed Eng Online*. 2021;20:1–13.
29. Shahla A, Charehsaz S, Hamzeh ZA. EVALUATION OF ANATOMIC PARAMETERS ON KNEE OSTEOARTHRITIS. 2007.
30. Seki K, Seki T, Siigi E, Imagama T, Yamabe T, Sakai T. Comparing inter-and intraobserver reliability between two-dimensional and three-dimensional measurements in the tibial component position of unicompartmental knee arthroplasty. *Acta Orthop Belg*. 2023;89:316–325.
31. Marouane H, Shirazi-Adl A, Adouni M. Alterations in knee contact forces and centers in stance phase of gait: a detailed lower extremity musculoskeletal model. *J Biomech*. 2016;49:185–192.
32. Peters AE, Geraghty B, Bates KT, Akhtar R, Readioff R, Comerford E. Ligament mechanics of ageing and osteoarthritic human knees. *Front Bioeng Biotechnol*. 2022; 10, 954837.
33. Dehghan M, Bahmani M. Anatomical parameters associated with osteoarthritis of the knee joint. *Armaghane Danesh [Internet]*. 2014;19:462–469. Available from: <http://armaghanj.yums.ac.ir/article-1-183-en.html>.
34. Park G, Kim T, Forman J, Panzer MB, Crandall JR. Prediction of the structural response of the femoral shaft under dynamic loading using subject-specific finite element models. *Comput Methods Biomech Biomed Eng*. 2017;20:1151–1166.
35. Zheng K. *The Effect of High Tibial Osteotomy Correction Angle on Cartilage and Meniscus Loading Using Finite Element Analysis*. University of Sydney; 2014.
36. Trad Z, Barkaoui A, Chafra M, Tavares JMRS. *FEM Analysis of the Human Knee Joint: A Review*. Springer; 2018.
37. Krone R, Schuster P. An investigation on the importance of material anisotropy in finite-element modeling of the human femur. *SAE Technical Paper*. 2006-01-0064.
38. Klein KF, Hu J, Reed MP, Hoff CN, Rupp JD. Development and validation of statistical models of femur geometry for use with parametric finite element models. *Ann Biomed Eng*. 2015;43:2503–2514.
39. Thienkarochanakul K, Javadi AA, Akrami M, Charnley JR, Benattayallah A. Stress distribution of the tibiofemoral joint in a healthy versus osteoarthritis knee model using image-based three-dimensional finite element analysis. *J Med Biol Eng*. 2020; 40:409–418.
40. Daniela T, Marius C, Nicolae TD. Modeling and finite element analysis of the human knee joint affected by osteoarthritis. *Key Eng Mater*. 2014;601:147–150.
41. Kumar VA, Jayanthi AK. Finite element analysis of normal tibiofemoral joint and knee osteoarthritis: a comparison study validated through geometrical measurements. *Indian J Sci Technol*. 2016;9:S1.
42. Watanabe K, Mutsuzaki H, Fukaya T, et al. Simulating knee-stress distribution using a computed tomography-based finite element model: a case study. *J Funct Morphol Kinesiol*. 2023;8:15.
43. Mononen ME, Paz A, Liukkonen MK, Turunen MJ. Atlas-based finite element analyses with simpler constitutive models predict personalized progression of knee osteoarthritis: data from the osteoarthritis initiative. *Sci Rep*. 2023;13:8888.
44. Lin EC. Radiation risk from medical imaging. *Mayo Clin Proc Elsevier*. 2010; 1142–1146.
45. Guggenberger R, Pfirrmann CWA, Koch PP, Buck FM. Assessment of lower limb length and alignment by biplanar linear radiography: comparison with supine CT and upright full-length radiography. *Am J Roentgenol*. 2014;202:W161–W167.
46. Viceconti M, Davinelli M, Taddei F, Cappello A. Automatic generation of accurate subject-specific bone finite element models to be used in clinical studies. *J Biomech*. 2004;37:1597–1605.
47. Esrafilian A, Chandra S, Gatti AA, et al. An automated and robust tool for musculoskeletal and finite element modeling of the knee joint. *bioRxiv*. 2023: 2010–2023.
48. Kim S-J, Bae J-H, Lim HC. Factors affecting the postoperative limb alignment and clinical outcome after Oxford unicompartmental knee arthroplasty. *J Arthroplast*. 2012;27:1210–1215.
49. Pourzal R, Cip J, Rad E, et al. Joint line elevation and tibial slope are associated with increased polyethylene wear in cruciate-retaining total knee replacement. *J Orthop Res*. 2020;38:1596–1606.
50. Nissinen MT, Hänninen N, Prakash M, et al. Functional and structural properties of human patellar articular cartilage in osteoarthritis. *J Biomech*. 2021;126, 110634.